*Kinetics and Catalysis, Vol. 44, No. 2, 2003, pp. 233–246. Translated from Kinetika i Kataliz, Vol. 44, No. 2, 2003, pp. 250–265.*


# Adsorption and Reactions of $N_2O$ on Transition Metal Surfaces

**A. V. Zeigarnik**

*Zelinskii Institute of Organic Chemistry, Russian Academy of Sciences, Moscow, 119991 Russia*

Received June 24, 2002

**Abstract**—Data on the interaction of nitrous oxide with polycrystalline and low-index single crystal surfaces of transition metals (Cu, Ag, Pt, Pd, Ni, W, Ir, Rh, and Ru) are reviewed. The kinetics of $N_2O$ adsorption, desorption, and dissociation $N_2O$ on these surfaces, as well as the energetics and mechanisms of these processes, are considered. New calculated data on the energetics of nitrous oxide transformations on (111) single crystalline transition metal surfaces are reported.

## INTRODUCTION

The catalytic chemistry of nitrous oxide has attracted considerable attention among researchers due to the problems of environmental chemistry and $NO_x$ decomposition [1, 2]. Furthermore, $N_2O$ is an interesting oxidant that can be a source of one oxygen atom and a nitrogen molecule [3]. Nitrous oxide is also interesting from the standpoint of theoretical problems of catalysis. This is a linear molecule with multiple bonds whose coordination on bulk metals and single crystalline planes is poorly studied. There are many questions relevant to the kinetics of $N_2O$ decomposition on these surfaces. For instance, it is unclear why the (111) surfaces are inert toward $N_2O$ dissociation, whereas other planes and polycrystalline surfaces are active. This short review deals with the problems of kinetics and mechanisms of $N_2O$ adsorption, desorption, and decomposition. Note that there are much less data for $N_2O$ than for NO adsorption [4]. Problems related to the use of $N_2O_{ads}$ as an oxidant in catalytic and other reactions, the interaction of nitrous oxide with metal oxides, supported metal catalysts, zeolites, and other nonmetallic materials have been considered in other review papers [1–3].

## MOLECULAR VERSUS DISSOCIATIVE ADSORPTION OF $N_2O$

It is known that nitrous oxide adsorbs on many transition metal surfaces: tungsten, rhenium, ruthenium, rhodium, iridium, nickel, palladium, platinum, copper, and silver. Depending on the metal, surface coverage, and plane, molecular or dissociative adsorption

$$N_2O \longrightarrow N_2 + O_{ads}$$

can be observed. Only molecular adsorption was observed on the surfaces of Ir(111) at >84 K [5], Ag(111) at >83 K [6], Ag(110) at 30 K [7], Ni(111) at >85 K [8], Pt(111) at >50 K [9, 10], and on a layer of Pd(111) on Ta(110) at >95 K [11].

Nitrous oxide poorly dissociates on the Cu(100) surface [7, 12] at low temperatures. According to [13], nitrous oxide does not adsorb on the Cu(100) and Cu(111) surfaces at 100 K even upon an exposure of 1000 Langmuir (L). At higher temperatures (>300 K) and substantial exposures (~$10^6$ L), $N_2O$ dissociates on the Cu(100) and Cu(111) surfaces, but molecular adsorption of nitrous oxide has not been observed. At 573 K and $10^{-4}$ Torr, the probability of $N_2O$ dissociation on the Cu(111) surface is estimated as $10^{-5}$ [12]. Thus, the absence of apparent molecular adsorption at low temperatures does not exclude dissociative adsorption at high temperatures.

Using the method of thermal desorption spectroscopy (TDS), chemisorbed and multilayer physisorbed nitrous oxide has been observed. According to TDS data, the binding energies of multilayer and submonolayer $N_2O$ are rather close. Physically adsorbed $N_2O$ desorbs from the Ir(111) surface at 93 K (multilayer adsorption) and chemisorbed $N_2O$ desorbs at 102 K (<1 monolayer, ML) [5]. Similar data have been reported for Ag(111) [6]. For this surface, two thermal desorption peaks were observed: at 98 K (multilayer adsorption) and 94–102 K (chemisorbed $N_2O$). On the Ni(111) surface, $N_2O$ weakly adsorbs without dissociation and forms three different species assigned to (a) multilayer adsorption (a desorption peak at ~70 K), (b) monolayer adsorption (a desorption peak desorbs at ~92 K), and (c) submonolayer adsorption (~0.1 ML, a desorption peak at ~100 K) [8]. In the case of multilayer adsorption on Pt(111), $N_2O$ desorbs at 86 K [9]. Kiss *et al.* [10] observed two thermal desorption peaks of $N_2O$: at 75–87 K (multilayer adsorption) and 97–102 K (chemisorption).

The adsorption of $N_2O$ with dissociation into molecular nitrogen and atomic oxygen occurs on the surfaces of Pd(110) at 95 K and even lower temperatures [14–16], Ir(110) in the temperature range 350–500 K [17], Rh(110) at 200–573 K [18], Ni(110) at 323–873 K [19], Cu(110) at >90 K [13, 20, 21], Ru(0001) at >83 K [22–25], and Rh(100) at 530–680 K [26]. According to

0023-1584/03/4402-0233$25.00 

Onchi and Farnsworth [27], the probability of nitrous oxide dissociation at 473–573 K on the Ni(100) surface is rather low and can be explained by the presence of defects. However, according to Hoffman and Hudson [28], nitrous oxide dissociates on the Ni(100) surface at 200–800 K. On the stepped surface Ni(755) = Ni(s)[6(111) × (100)], $N_2O$ dissociates at temperatures lower than 200 K [29], and steps are the active sites of dissociation. Nitrous oxide dissociation readily occurs on polycrystalline surfaces: iridium, palladium [30], platinum [31, 32], rhodium (even at room temperature) [33], and rhenium (from room temperature to 1200 K) [34]. It has been found that rhodium catalysts readily decompose $N_2O$ under catalytic conditions at 523–623 K [35], and oxygen is released to the gas phase. On the other hand, thermal desorption studies in a vacuum showed that atomic oxygen is stable on the rhodium surface up to temperatures as high as ~1100 K [35]. A mechanism has been proposed that explains this discrepancy [35]:

$$N_2O_{gas} \longrightarrow N_{2,\,gas} + O_{ads},$$
$$N_2O_{gas} \rightleftharpoons N_2O_{ads},$$
$$2O_{ads} \rightleftharpoons O_{2,\,gas},$$
$$N_2O_{ads} + O_{ads} \longrightarrow N_{2,\,gas} + O_{2,\,gas}.$$

In the case of dissociative adsorption, a mobile precursor model has been suggested [14, 26, 30–34]:

$$N_2O \rightleftharpoons N_2O_{ads} \longrightarrow N_{2,\,gas} + O_{ads}$$

or a model with two precursors $N_2O_{ads}$(I) and $N_2O_{ads}$(II) [19, 28]

$$N_2O \rightleftharpoons N_2O_{ads}(I) \longrightarrow N_{2,\,ads} + O_{ads},$$
$$N_{2,\,ads} \rightleftharpoons N_{2,\,gas},$$
$$N_2O \rightleftharpoons N_2O_{ads}(II),$$
$$N_2O_{ads}(I) \rightleftharpoons N_2O_{ads}(II).$$

The existence of a precursor is usually judged by the independence of the initial sticking coefficient of the surface coverage [14].

Molecular adsorption can be observed in parallel with the dissociative adsorption. This has been convincingly demonstrated for surfaces that are moderately active toward nitrous oxide dissociation [22–25]. Haq and Hodgson [14] proposed a mechanism according to which $N_2O$ either weakly adsorbs on the surface to form a surface intermediate, which is a precursor of dissociation, or forms a more strongly adsorbed $N_2O$ species.

On some active metals (such as tungsten and ruthenium), the N–N bond is cleaved. On the W(110) surface, $N_2O$ dissociatively adsorbs at room temperature and forms atomic nitrogen and atomic oxygen [24]. Molecular nitrogen does not desorb [36]. Weinberg and Merrill [37] showed that nitrous oxide adsorbs on the W(100) surface at 295 and 500 K, and both of its bonds are cleaved. When the substrate is heated upon $N_2O$ adsorption, two $N_2$ desorption peaks are observed: one is assigned to adsorbed molecular nitrogen and the other is assigned to atomic nitrogen. The Ru($10\bar{1}0$) surface is also very active toward $N_2O$ dissociation [38]. The cleavage of the N–O bond with the formation of adsorbed atomic oxygen and gaseous nitrogen occurs at room temperature. At higher temperatures, all bonds are cleaved in $N_2O$ to form atomic oxygen and atomic nitrogen on the surface.

On some of the surfaces studied, $N_2O$ adsorption has not been detected. Thus, on the Rh(111) surface, $N_2O$ adsorbs neither molecularly nor dissociatively at temperatures from room temperature to 900 K [18]. Li and Bowker [18] assumed that adsorption requires overcoming a high activation barrier, but this assumption seems highly improbable because the activation energy of adsorption is usually low or equal to zero on clean surfaces. According to Spitzer and Luth [13], in the temperature range 90–300 K, nitrous oxide is not adsorbed in Cu(111). We cannot exclude that molecular adsorption of $N_2O$ is possible on almost all surfaces, but researchers do not always explore wide ranges of temperatures and exposures.

The incompleteness of data prevents us from revealing the trends of activity toward $N_2O$ adsorption and dissociation across the periodic table (see Table 1). However, we see a pronounced structural sensitivity of nitrous oxide decomposition. Polycrystalline and fcc (110) surfaces are more active toward nitrous oxide dissociation than the (100) surfaces. The latter are more active than (111). On the (111) surfaces, adsorption may not occur or is molecular. The only fcc (110) surface studied on which no $N_2O$ dissociation was observed is Ag(110) [7]. On most metals and surfaces (except for such active surfaces as W(110) and Ru($10\bar{1}0$)), the dissociation occurs with N–O bond scission and without N–N bond scission.

Thus, fcc (110) surfaces and some fcc (100) and (111) surfaces, bcc W(100), W(110), and supposedly W(111) surfaces, various hcp surfaces of Ru, and polycrystalline surfaces are active in nitrous oxide dissociation. On the fcc surfaces (110), electron-induced $N_2O$ dissociation (Ag(111) [6]) and dissociation induced by ultraviolet irradiation (Pt(111) [10]).

Let us now consider some of the active surfaces in more detail.

### *Fcc (110) Surfaces*

On the surfaces of Ni(110), Pd(110), Rh(110), Ir(110), and Cu(110), nitrous oxide dissociates to form adsorbed atomic oxygen and gaseous nitrogen.

On Pd(110) at 85, the sticking coefficient remains constant up to 0.8 ML and then drastically decreases to zero at 1 ML [14]. When the reaction is completed (when adsorption ends due to site blocking), 0.15 ML of the surface is filled with atomic oxygen and 0.85 ML is filled with adsorbed $N_2O$ (the number of adsorption

**Table 1.** Comparison of the activities of metals and their surfaces

| Group / Period | VIB | VIIB | VIII | | | IB |
|---|---|---|---|---|---|---|
| 4 | Cr<br>No data | Mn<br>No data | Fe<br>No data | Co<br>No data | Ni<br>(110) 323–873 K dissociative<br>(100) 200–800 K dissociative<br>(111) <100 K molecular | Cu<br>(110) >90 K dissociative<br>(100) 90–300 K molecular<br>>300 dissociative<br>(111) 90–300 K no adsorption,<br>>300 dissociative |
| 5 | Mo<br>No data | Tc<br>No data | Ru<br>(0001)<br>75–115 K: $N_2O$<br>>115 K: $N_2$ + O<br>$(10\bar{1}0)$ 150–295 K: $N_2$ + O<br>>295 K : N + O | Rh<br>(110) 200–573 K dissociative<br>(100) 530–680 K dissociative<br>(111) 295–900 K no adsorption<br>(poly) dissociative | Pb<br>(110) > 85 dissociative<br>(100) no data<br>(111) > 95 K molecular<br>(poly) dissociative | Ag<br>(110) 30 K molecular<br>(100) no data<br>(111) > 83 K molecular |
| 6 | W<br>(110) > 100 K dissociative (to N and O)<br>(100) 295–500 K dissociative (to N and O)<br>(111) No data | Re<br>(poly) 295–1200 K dissociative | Os<br>No data | Ir<br>(110) 350–500 K dissociative<br>(100) no data<br>(111) > 84 K molecular<br>(poly) dissociative | Pt<br>(110) no data<br>(100) no data<br>(111) >75 K molecular<br>(poly) dissociative | Au<br>No data |

Note: Poly denotes a polycrystalline surface.

sites is counted as the number of adsorbates divided by the number of surface atoms). On a clean Pd(110) surface, $N_2O$ initially dissociates very efficiently (~60% of nitrous oxide consumed), then this reaction channel reduces to ~5% when the surface coverage reaches 0.5 ML. Further adsorption of $N_2O$ occurs without dissociation. At higher temperatures (300, 473, and 573 K), the sticking coefficient decreases more rapidly as $N_2O$ is consumed. The initial accumulation of the precursor is not observed. Atomic oxygen and desorbing nitrogen are formed. The reaction ceases when the surface becomes covered with 0.5 ML of atomic oxygen. At this moment, regular overlayer Pd(110)-c$(2 \times 4)$O structures are formed (Fig. 1).

Analogous results have been obtained for the Rh(110) surface [18]. At 198, 440, and 573 K, the sticking coefficient decreases to zero at 0.5 ML O. The initial portions of the plots of the sticking coefficient versus surface coverage contained plateaus. The independence of the sticking coefficient on the surface coverage during an initial period points to the formation of a precursor as in the case of Pd(110). At 198 K, saturation was observed at 0.35 ML and a decrease in the sticking coefficient was more rapid. When adsorption was completed, no ordered overlayer structure below room temperature was detected. At 573 K, an incompletely formed $(2 \times 2)$p2mg structure was observed by LEED.

It is known for the Cu(110) surface that at 90 K nitrous oxide adsorption is initially dissociative, whereas when the surface coverage by oxygen reaches 0.25 ML, both molecular and dissociative adsorption occur. The reaction is completed when the surface coverage by oxygen reaches 0.5 ML [13]. According to UV photoemission spectroscopy, $N_2O$ desorption occurs at 115 K. These data agree with those obtained earlier: at room temperature, the initial sticking coefficient is 0.15 and then it decreases to zero at saturation at 0.5 ML [39].

In the case of $N_2O$ adsorption on Ni(110) [19], the initial sticking coefficient decreases from 0.97 to 0.52 with an increase in the temperature from 323 to 873 K. Data obtained in [19] point to the formation of a mobile precursor. The surface saturates at an oxygen coverage of 1/3 ML.

The adsorption of $N_2O$ on Ir(110) has been poorly studied [17].

Data on the temperature dependences of the initial sticking probabilities are summarized in Fig. 2: above room temperature the activity of the (110) surface

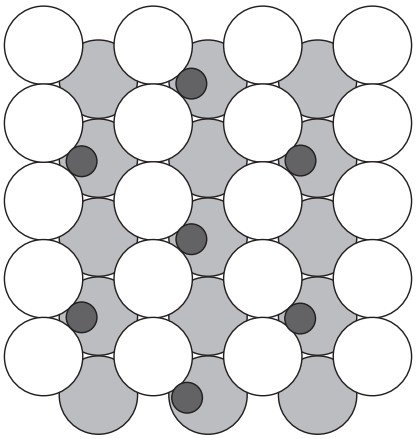

**Fig. 1.** Ordered overlayer c(2 × 4)O structures on the fcc (110) surface (small circles denote oxygen atoms, large light circles denote metal atoms on the surface, and large dark circles denote metal atoms in the second layer).

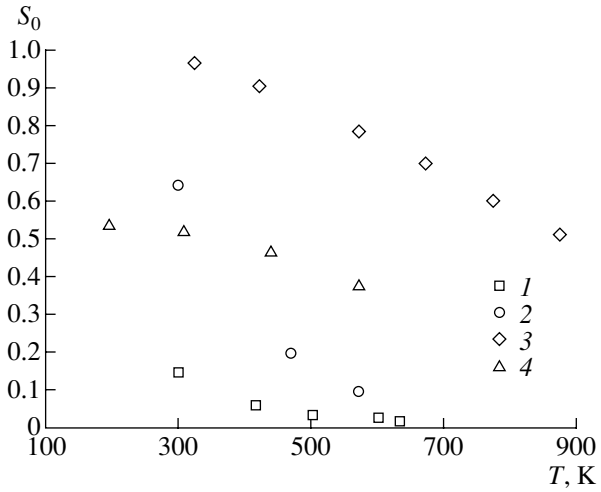


**Fig. 2.** Temperature dependences of the initial sticking coefficients for (*1*) Cu(110), (*2*) Pd(110), (*3*) Ni(110), and (*4*) Rh (110).

decreases in the following series: Ni(110) > Rh(110) > Pd(110) > Cu(110).

### *Fcc Surfaces (100) and (111)*

On the Cu(111) surface, the dissociation probability is very low: $10^{-9}$ at room temperature and it increases with an increase in the temperature, whereas the surface saturates at $\theta_O = 0.45$.

Nitrous oxide partly dissociates on a Ni(100) surface. The probability of dissociation at 473–573 K is rather low and can be explained by the presence of defects [40]. Hoffman and Hudson [28] studied this process on Ni(100) at 200–800 K in more detail. They found that, as in the case of Ni(110), the dissociation is described by a precursor model. The long exposure of the sample to $N_2O$ leads to the saturation of the surface by atomic oxygen up to the maximal coverages, which depend on the temperature (0.25 ML at 350–500 K). Nondissociated $N_2O$ molecules are also present on the surface.

### *Ru(0001) and Ru(10$\bar{1}$0) Surfaces*

On an Ru(0001) surface, $N_2O$ adsorbs at 75 K [23]. Sample heating at low surface coverages led to the decomposition of $N_2O$ and to the desorption of $N_2$ to the gas phase at 110–120 K. At higher initial surface coverages in this temperature range, $N_2O$ desorption also occurred [23]. The adsorption of $N_2O$ on Ru(0001) has also been studied by Huang *et al.* [25]. At low exposures, one thermal desorption peak was observed at 129 K, which steadily switched toward higher temperatures (145 K) as the surface coverage increased. That is, the binding strength of $N_2O$ increased with an increase in the surface coverage. With an increase in exposure, two additional peaks were observed (at 160–165 K and 116–123 K). When $N_2O$ was adsorbed at 100 K, $N_2$ was not detected in the desorption products. One of the thermal desorption peaks (at 160–165 K) was assigned to $N_2O$ coadsorbed with atomic oxygen. This peak starts to reveal itself with an increase in the exposure.

The Ru(10$\bar{1}$0) surface is very active toward nitrous oxide decomposition [41]. Most of nitrous oxide dissociates on this surface. It was found that $N_2O$ occurs in two directions. One of them is N–O bond cleavage with the formation of atomic oxygen on the surface and the release of molecular nitrogen into the gas phase (this reaction occurs in the range from 150 K to room temperature); the other direction is the cleavage of all bonds in $N_2O$ with the formation of atomic nitrogen and atomic oxygen on the surface (this occurs at higher temperatures). It was found that preadsorbed oxygen saturating the surface contaminates it, and dissociation does not occur. The amount of desorbed molecular nitrogen after nitrous oxide adsorption strongly depends on temperature and passes through a maximum near 600 K. The amount of desorbing molecular oxygen depends on temperature in a radically different manner. Two maximums are observed (at ~415 and 1100 K) and a minimum at 600 K. Moreover, when the surface is saturated with the equivalent amount of oxygen using $O_2$ rather than $N_2O$ as a source, approximately two times more gaseous oxygen is formed in thermal desorption. Klein and Siegel [41] concluded that there are two pathways of $N_2O$ activation, one of which is the formation of atomic nitrogen at high temperatures. However, they did not consider the reaction $N_2O_{ads} + O_{ads} \longrightarrow N_{2,\,gas} + O_{2,\,gas}$ as a possible source of molecular nitrogen.

### *W(110) and W(100) Surfaces*

When nitrous oxide is adsorbed on W(110) [36] at 100 and 300 K, the surface saturates at 0.5–0.75 ML. At 300 K, only dissociative adsorption occurs, whereas at 100 K molecular adsorption is also possible. Upon saturation of the surface due to nitrous oxide dissociation, the N : O ratio is lower than in the $N_2O$ molecule (especially at higher temperatures). This fact points to the partial desorption of $N_2$. Nitrous oxide readily forms several layers on the surface.

### *Polycrystalline Surfaces*

Nitrous oxide usually dissociates on polycrystalline surfaces. Information obtained on most of them is obtained by kinetic studies. Thus, Redmond studied nitrous oxide decomposition on the filaments of iridium, palladium [30] and platinum [31]. The following rate law was proposed to describe the decomposition of $N_2O$ on platinum filaments

$$-\frac{dP_{N_2O}}{dt} = k_{app}P_{N_2O}P_{O_2}^{-0.5}, \quad (1)$$

where $k_{app}$ is the apparent rate constant. This rate law was derived from the following mechanism

$$N_2O \rightleftharpoons N_2O_{ads},$$
$$N_2O_{ads} \longrightarrow N_2 + O_{ads},$$
$$O_{ads} \rightleftharpoons 1/2O_2.$$

Redmond assumed that the rate-determining step is the dissociation of $N_2O$ and obtained the following equation:

$$-\frac{dP_{N_2O}}{dt} = \frac{k_0K_1P_{N_2O}}{1 + K_1P_{N_2O} + K_2P_{O_2}^{1/2}}, \quad (2)$$

where $k_0$ is the rate constant of $N_2O$ dissociation, $K_1$ and $K_2$ are the equilibrium constants of $N_2O$ and $O_2$ adsorption. Then, assuming that $K_1P_{N_2O} \ll K_2P_{O_2}^{1/2}$ and $1 \ll K_2P_{O_2}^{1/2}$, Eq. (2) transforms into Eq. (1). Redmond obtained the value of the apparent activation energy ($E_{app}$ = 32 kcal/mol), which agrees with earlier data (±1 kcal/mol). The heat of oxygen adsorption on platinum was also estimated: $Q_2$ = 18 kcal/mol. Then, we can obtain from the expression $E_{app} + Q_1 - Q_2 = E_{diss}$, which can be derived from Eqs. (1) and (2), that $E_{diss} = 14 + Q_1$, where $Q_1$ is the heat of $N_2O$ adsorption. In my opinion, the above assumptions are incorrect. The reaction of $N_2O$ decomposition has a low activation energy, which is close to $Q_1$.

The decomposition of $N_2O$ on iridium filaments is described by Eq. (1) at 1281–1617 K [30]. The apparent activation energy is ~40 kcal/mol. The addition of gaseous oxygen poisons the reaction.

The decomposition of nitrous oxide on palladium is described by the following rate law:

$$-\frac{dP_{N_2O}}{dt} = k_0K_1P_{N_2O}(1 + K_2P_{O_2})^{-1},$$

where $k_0$ is the intrinsic rate constant of decomposition and $K_1$ and $K_2$ are the equilibrium constants of $N_2O$ and $O_2$ adsorption. The apparent activation energy is ~30 kcal/mol. In the case of palladium, gaseous oxygen also poisons the reaction. The activity of metals in $N_2O$ decomposition decreases in the series Pd > Pt > Ir.

Similar data for platinum were obtained in [32] for the temperature range 773–1473 K. At 773–873 K, the rate of $N_2O$ decomposition is proportional to the partial pressure of nitrous oxide and is in inverse proportion to the oxygen pressure. At temperatures above 1173 K, there is a limit when retardation by oxygen is no longer effective. It was assumed that oxygen is removed from the surface via the reaction between atomic oxygen and nitrous oxide.

In addition to the interaction of gaseous nitrous oxide with the surface, adsorbed nitrous oxide can be obtained from NO on the surfaces of various metals. Thus, nitrous oxide is formed on Mo(110) at 90 K [4], W(110) at <150 K [42], Cu(110) at 90 K [4], Cu(100) [43], Cu(111) at 85 K [4, 44], Ag(111) at 100 K [4, 45–50], Pd(110) [51, 52], and Ag/Ru(0001) [53].

There is no general agreement regarding the mechanism of $N_2O$ formation. It likely that mechanisms may differ depending on the reaction conditions and the surface. Possible pathways of $N_2O$ formation can be described by the following reactions:

$$NO_{ads} + NO_{ads} \longrightarrow NO_{ads} + N_{ads}$$
$$+ O_{ads} \longrightarrow N_2O_{ads} + O_{ads},$$
$$NO_{ads} + NO_{ads} \longrightarrow (NO)_{2,\,ads} \longrightarrow N_2O_{ads} + O_{ads},$$
$$NO_{ads} + NO_{ads} \longrightarrow N_2O_{ads} + O_{ads}.$$

## EFFECT OF COADSORBED OXYGEN

Coadsorbed oxygen atoms play an important role in nitrous oxide decomposition, whereas molecular oxygen desorbing at high temperatures from polycrystalline surfaces retards the reaction. Adsorbed atomic oxygen blocks active sites on the catalyst surface. Its binding to the surface is much stronger than the binding of adsorbates and, therefore, it is the least mobile. The binding energy of atomic nitrogen is even higher, but it is only formed on the most active surfaces. The formation of atomic oxygen leads to site blocking whereas nitrous oxide dissociation requires many free sites on the surface. Due to site blocking, bending or inclination of $N_2O$ toward the surface, which is required for dissociation, is hindered and $N_2O$ remains in the molecularly adsorbed state. Moreover, lateral interactions between the atomic oxygen and $N_2O$ are attractive and lead to an increase in the activation energy and temperature of

nitrous oxide desorption. Let us consider some data that point to $N_2O$ stabilization due to coadsorbed oxygen atoms.

Spitzer and Luth [13] compared data obtained by thermal desorption from a clean Cu(110) surface and a surface covered with 0.5 ML of atomic oxygen. In the latter case, the desorption temperature was higher, suggesting that nitrous oxide molecules are bound more strongly if there are coadsorbed oxygen atoms. That is, the lateral interactions of $N_2O$ and O are attractive.

The stabilization of $N_2O$ by atomic oxygen, which prevents $N_2O$ from decomposition, was detected by thermal desorption mass spectrometry in the case of Ir(110) [17]. An increase in the apparent activation energy of nitrous oxide dissociation on Cu(110) was demonstrated by Auger spectroscopy [39].

On Ni(755) [29], the decomposition of $N_2O$ occurs on steps. When they are occupied by atomic oxygen formed in this reaction, the decomposition of $N_2O$ discontinues. Moreover, on clean steps, the reaction occurs at 105 K and $N_2$ desorbs at 170 K. When steps are partly filled with atomic oxygen, $N_2O$ dissociates at 120 K and $N_2$ desorbs at this temperature. These data suggest that the activation energy of $N_2O$ decomposition increases as oxygen is accumulated at the active sites on the surface. Molecular nitrogen starts to desorb more readily due to repulsion between $N_2$ and atomic oxygen or due to a change in the mechanism of nitrous oxide decomposition.

On the Ni(110) surface, a decrease in the sticking coefficient (and the rate of dissociation) was observed with an increase in the surface coverage by oxygen and described by the formula [19]

$$S = S_0\left[1 + \frac{k'_d}{k_d + k_r}\left(\frac{\theta/\theta_{sat}}{1-\theta/\theta_{sat}}\right)\right]^{-1}, \qquad (3)$$

where $S_0$ is the initial sticking coefficient; $k'_d$ is the desorption rate constant of spectator $N_2O$, which does not dissociate but can be transformed into a precursor; $k_d$ is the rate constant of precursor desorption; and $k_r$ is the rate constant of $N_2O_{ads}$ dissociation into $N_{2,\,ads}$ and $O_{ads}$. That is, oxygen rapidly poisons the metal surface and the reaction is completed at a saturation coverage $\theta_{sat}$ equal to 1/3 ML. An analogous formula describes well the dissociative adsorption of $N_2O$ on Cu(111) [12].

Scholten *et al.* [54] showed that the reaction of $N_2O$ decomposition can be used to determine the specific surface area of polycrystalline silver samples. They showed that the apparent activation energy of nitrous oxide decomposition strongly depends on the surface coverage by oxygen: each next 0.1 ML (calculated per one metal atom on the surface) corresponds to an increase in the activation energy by ~10 kcal/mol.

However, there are some data that contradict the role of oxygen described above. Thus, on the clean Ni(100) surface, the binding energy of nitrous oxide is 1.5 kcal/mmol higher than on a surface covered with 0.25 ML of atomic oxygen [28]. This fact provides negative evidence for attractive lateral interactions between atomic oxygen and nitrous oxide.

On Ru(0001), $N_2O$ adsorption is also sensitive to the presence of preadsorbed oxygen [25]. Even a small amount of preadsorbed oxygen leads to an increase in the $N_2O$ binding strength. However, the dependence of the stabilization efficiency of molecular $N_2O$ adsorption on the surface coverage is not monotonic. After some optimum (at 0.1 ML), oxygen stops stabilizing molecular $N_2O$ and starts to weaken its binding. The presence of oxygen also favors $N_2O$ decomposition. The sticking coefficient on a surface with preadsorbed oxygen ($\theta_O = 0.15$) is 2.7 higher than on a clean surface. This example shows that it is sometimes insufficient to compare the sticking probabilities on surfaces with and without preadsorbed oxygen. Rather, it is important to determine how oxygen formed in the reaction affects the nature of $N_2O$ binding.

## EFFECTS OF OTHER COADSORBATES

Shi and White [55] showed that, on an Ru(0001) surface with preadsorbed carbon, the rate of nitrous oxide dissociation noticeably decreases with an increase in the surface coverage by carbon. Thus, the initial dissociation probability of $N_2O$ decreases by 90% when the coverage by carbon is as small as 0.09 ML. However, the high activity of a metal can be restored by heating the sample in the presence of nitrous oxide or oxygen and further recombinative desorption of atomic oxygen. A decrease in the activity of C/Ru(0001) compared to clean Ru(0001) is associated with site blocking. The decomposition of $N_2O$ is much more sensitive to the presence of coadsorbates than the dissociative adsorption of oxygen. The presence of preadsorbed deuterium atoms on an Ru(0001) surface leads to a decrease in the temperature of $N_2O$ desorption. That is, lateral interactions between $N_2O_{ads}$ and $D_{ads}$ are repulsive [25]. The interactions between $CO_{ads}$ and $N_2O_{ads}$ are repulsive as well [25].

## GEOMETRY OF ADSORBED NITROUS OXIDE

The geometry of adsorbed nitrous oxide has been studied very poorly. It is clear that the geometry of adsorbed $N_2O$ and site preference depend on the type of metal, the face of the crystal lattice, an the surface coverage with various adsorbates and their relative concentrations. Most researchers seem to agree that $N_2O$ adsorbs via the terminal nitrogen atom. Data obtained by various experimental and theoretical methods are summarized in Table 2.

## ENERGETICS

Data on the energetics of nitrous oxide adsorption and dissociation are scarce and contradictory. There is

**Table 2.** Data on the geometries of the $N_2O$ adsorption states

| Surface | Proposed geometry | Method | Ref. |
|---|---|---|---|
| Cu(110) 1 ML | Normal to the surface or at an angle close to 90° | Electron energy loss spectroscopy (EELS) | [13] |
| Cu(100) 1 ML | 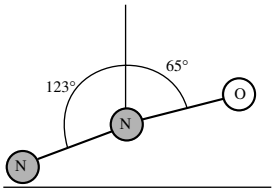 | Near-edge X-ray adsorption fine structure (NEXAFS) | [7] |
| Cu(100) 0.5 ML | 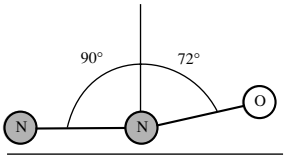 | NEXAFS | [7] |
| Ag(100) (0.5 and 1 ML) | 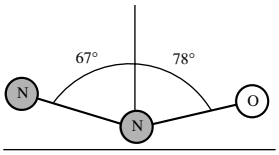 | NEXAFS | [7] |
| Pt(111) | 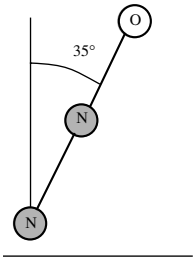 | EELS | [9] |
| Ni(111) (1 ML) | 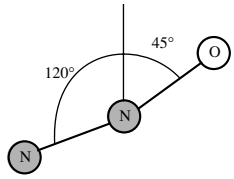 | NEXAFS | [8] |
| Pd(111)–c(2 × 2) 0.5 ML | 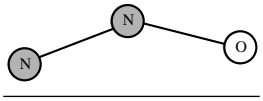 <br>Most preferable configuration<br>∠PdNN = 130°, ∠NNO = 156°, ∠NOPd = 116° | DFT calculation (GGA–PBE) | [63] |
| Pd(110)–c(2 × 2) 0.5 ML | 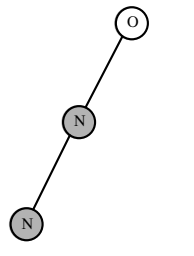 <br>∠PdNN = 150°, ∠NNO = 179°<br>One of the favorable configurations | DFT calculation (GGA–PBE) | [63] |
| Ru(0001) | At low surface coverages, the configuration is linear, normal to the surface with binding via the terminal nitrogen atom; at high coverages, the molecules is inclined | High-resolution electron energy loss spectroscopy (HREELS) | [23] |

**Table 3.** Binding energies of atomic adsorbates (in kcal/mol) on various surfaces

| $Q$ | Pt | Pd | Re | Rh | Ir | Ni | Au | Ag | Cu |
|---|---|---|---|---|---|---|---|---|---|
| $Q_{0N}$ | 69.6 | 78.0 | 85.2 | 69.6 | 76.2 | 81.0 | 58.2 | 60.0 | 69.0 |
| $Q_{0O}$ | 51.0 | 52.3 | 75.0 | 61.2 | 55.8 | 69.0 | 45.0 | 48.0 | 61.8 |
| $Q_N$ for (111)/(0001) | 116.0 | 130.0 | 142.0 | 116.0 | 127.0 | 135.0 | 97.0 | 100.0 | 115.0 |
| $Q_N$ for (100) | 121.8 | 136.5 | 149.1 | 121.8 | 133.4 | 141.8 | 101.9 | 105.0 | 120.8 |
| $Q_N$ for (110) | 125.3 | 140.4 | 153.4 | 125.3 | 137.2 | 145.8 | 104.8 | 108.0 | 124.2 |
| $Q_O$ for (111)/(0001) | 85.0 | 87.2 | 125.0 | 102.0 | 93.0 | 115.0 | 75.0 | 80.0 | 103.0 |
| $Q_O$ for (100) | 89.3 | 91.5 | 131.3 | 107.1 | 97.7 | 120.8 | 78.8 | 84.0 | 108.2 |
| $Q_O$ for (110) | 91.8 | 94.1 | 135.0 | 110.2 | 100.4 | 124.2 | 81.0 | 86.4 | 111.2 |

only one paper reporting the energetics of $N_2O$ adsorption calculated by density functional theory (DFT). Using this method in the GGA–PBE approximation, the binding energy of nitrous oxide on a Pd(110)–$c(2\times2)$ surface (0.5 ML $N_2O$) was calculated. The surface was modeled by a five-layer slab [63]. It was found that at this coverage the most energetically favorable is on-top binding via the terminal nitrogen atom. Two favorable geometries are shown in Table 2. Another favorable configuration is linear, normal to the surface. The calculated binding energies are 0.39 eV (9.0 kcal/mol) for vertical inclined binding via the nitrogen atom with bending, 0.38 eV (8.8 kcal/mol) for horizontal binding of a bent $N_2O$ molecule via terminal atoms on two palladium atoms in the direction [001] along the surface, and 0.36 eV (8.3 kcal/mol) for vertical binding along the surface normal via the nitrogen atom. Based on theoretical and experimental data on the spatial distribution of desorbing $N_2$ molecules in the decomposition of $N_2O$ on Pd(110), Kokalj *et al*. [63] assumed that a nitrous oxide molecule first adsorbs in a configuration close to vertical, then a molecular precursor is formed in which a terminal oxygen atom is close to the surface. After N–O bond cleavage, $N_{2,\,ads}$ and $O_{ads}$ are formed and molecular nitrogen desorbs. The angular distribution of desorbing nitrogen molecules points to the formation of intermediate $N_{2,\,ads}$.

Proceeding from data on the temperature dependence of the initial sticking coefficient, Sau and Hudson [19] concluded that at the zero-coverage limit on Ni(110), the activation energy of $N_2O$ desorption ($E_d$) is higher than the activation energy of dissociation ($E_{diss}$) by 3.7 kcal/mol. An analogous study of the Pd(110) surface at zero coverage gives the value $E_d - E_{diss}$ = 3.3 kcal/mol [14], but this value was obtained using only three values of $S_0$ at different temperatures, whereas the fourth value (at 85 K) fell out of the series and was excluded from consideration. The activation energy of $N_2O_{ads}$ dissociation, estimated from the temperature of the thermal desorption peak, was 9 kcal/mol [51].

For a Cu(111) surface, Habraken *et al.* [12] obtained that $E_d - E_{diss}$ = 10.4 kcal/mol, although they mistakenly assigned this value to $E_{diss}$. The upper estimate of the adsorption heat of $N_2O$ on Cu(100) at a presumptive surface coverage of 0.5 ML O + 0.5 ML $N_2O$ was obtained: 6 kcal/mol [43]. On a Cu(110) surface, the value $E_d - E_{diss}$ is 2 kcal/mol, according to data on the temperature dependence of the sticking coefficient [39].

On a Pt(111) surface, $N_2O$ adsorbs in molecular form [9]. The initial heat of adsorption estimated from thermal desorption data is 5.6 kcal/mol and increases to 6.05 kcal/mol due to the attractive lateral interactions of adsorbed molecules as the surface is covered with $N_2O$ molecules until saturation at 0.7 ML. In the case of multilayer adsorption, the heat is close to 5.2 kcal/mol.

On a clean Ni(100) surface [28], the kinetic parameters of steps were determined for the model with two precursors based on a study of the reaction on a clean surface and on a surface with preadsorbed oxygen. The value $E_d - E_{diss}$ = 3.7 kcal/mol obtained earlier for Ni(110) was used [19]. On a clean Ni(100) surface, the activation energy of desorption is 6.2 kcal/mol (and the preexponential factor is $10^{12.3\pm3.2}$). The activation energy of desorption on 0.25 ML O/Ni(100) is 4.7 kcal/mol (the preexponential factor is $10^{10.5\pm2.2}$). The activation energy of dissociation is 2.5 kcal/mol [28].

Useful information on the energetics of adsorption of species participating in the reactions considered above and on the activation energies of these surface reactions can be calculated using the method of unity bond index–quadratic exponential potential (UBI–QEP). These calculations are discussed below. The systems under consideration have not been calculated before on such a scale. The essence of the method and its applications were described in detail in [56–58].

## UBI–QEP ESTIMATES OF ADSORBATE BINDING ENERGIES AND ACTIVATION ENERGIES OF STEPS

### *Adsorbate Binding Energies*

The method makes use of the data on the energies of two-center metal–adsorbate bonds $Q_{0A}$ (A = N, O) tested in other system (Table 3) [57]. Table 3 also lists the values of binding energies of atomic adsorbates, which can be calculated from the energies of two-center

**Table 4.** Calculated binding energies of NO ($Q_{NO}$, in kcal/mol) on various surfaces

| Surface | Pt | Pd | Re | Rh | Ir | Ni | Au | Ag | Cu |
|---|---|---|---|---|---|---|---|---|---|
| (111)/(0001) | 27.8 | 34.4 | 40.5 | 27.8 | 32.9 | 36.9 | 19.9 | 21.1 | 27.4 |
| (100) | 28.8 | 35.7 | – | 28.8 | 34.1 | 38.3 | 20.5 | 21.7 | 28.3 |
| (110) | 29.4 | 36.5 | – | 39.4 | 34.9 | 39.2 | 20.8 | 22.1 | 28.9 |

**Table 5.** Calculated binding energies of $N_2$, $O_2$, and $(NO)_2$ (in kcal/mol) on various surfaces

| Adsorbate | Pt | Pd | Re | Rh | Ir | Ni | Au | Ag | Cu |
|---|---|---|---|---|---|---|---|---|---|
| $N_2$ | 10.8 | 13.4 | 15.8 | 10.8 | 12.8 | 14.4 | 7.7 | 8.1 | 10.6 |
| $O_2$ | 10.6 | 11.1 | 21.5 | 14.8 | 12.5 | 18.5 | 8.4 | 9.5 | 15.1 |
| $(NO)_2$ | 43.9 | 53.1 | 61.5 | 43.9 | 51.1 | 56.6 | 32.4 | 34.1 | 43.3 |

bonds in the framework of the UBI–QEP method according to the formula

$$Q_A = Q_{0A}(2 - 1/n), \quad (4)$$

where $n$ is the number of metal atoms to which atom A binds. In the case of an atomic adsorbate on an fcc (111) or hcp (001) surface, $n = 3$. For fcc (100) and (110) surfaces, $n = 4$ and 5, respectively.

In the systems under consideration, reactions that occur or may occur involve the following surface species: $N_2O_{ads}$, $O_{ads}$, $N_{ads}$, $NO_{ads}$, $N_{2,\,ads}$, $(NO)_{2,\,ads}$, and $O_{2,\,ads}$. We use the binding energies of atomic adsorbates $O_{ads}$ and $N_{ads}$ as initial data. Other binding energies are calculated by the UBI–QEP method.

**NO.** At low coverages, NO usually binds via the nitrogen atom to the surface at hollow sites between three metal atoms on fcc (111) and hcp (001) surfaces or between four metal atoms on fcc (110) and (100) surfaces [4, 59]. In the zero-coverage limit, the binding energy of NO is calculated by the formula

$$Q_{NO} = \frac{Q_{0N}^2}{Q_{0N}/n + D_{NO}}, \quad (5)$$

where $D_{NO}$ is the bond energy in NO (151 kcal/mol). The results of calculations of NO binding energies on various surfaces are summarized in Table 4. As can be seen, the differences in the binding energies on various surfaces of the same metal are small.

**$N_2$.** Adsorbed molecular nitrogen can be in two configurations, one of which is vertical or inclined to the surface (binding via one nitrogen atom), and the other is horizontal (binding via two nitrogen atoms). The ground state is on-top vertical binding normal to the surface via one nitrogen atom. On the other hand, the binding energies of $N_2$ in both states are very low, and easy transitions between the two states are possible. The best approximation in the framework of the UBI–QEP method is the use of the formula for binding via two atoms (for homonuclear adsorbates):

$$Q_{N_2} = \frac{9Q_{0N}^2}{6Q_{0N} + 16D_{N_2}}, \quad (6)$$

where $D_{N_2}$ is the energy of the N–N bond (226 kcal/mol). The binding energies of molecular nitrogen are the same for all crystalline planes of the same metal.

**$O_2$.** For molecular oxygen adsorbed on the surface, we use a similar formula:

$$Q_{O_2} = \frac{9Q_{0O}^2}{6Q_{0O} + 16D_{O_2}}, \quad (7)$$

where $D_{O_2}$ is the energy of the O–O bond (119 kcal/mol).

**$(NO)_2$.** Nitric oxide dimers are characterized by a very weak N–N bond. Its energy is 2.87 kcal/mol [60]. This dimer binds to the surface via two nitrogen atoms, whereas oxygen atoms are directed upright at a certain angle [4]. For this case, a reasonable upper estimate of the binding energy is equal to the sum of binding energies of two NO molecules in the on-top state ($n = 1$).

Table 5 summarizes the results of calculations for $N_2$, $O_2$, and $(NO)_2$ binding in the zero-coverage limit.

**$N_2O$**. The calculation of $N_2O$ binding energy in the framework of the UBI–QEP method is more difficult compared to the calculations of other adsorbates considered here [58]. Another problem is that the UBI–QEP method does not allow one to analyze which of the adsorption states is preferable by comparing the results obtained by different formulas.

The most probable ground state of $N_2O$ is its orientation along the surface normal or at some angle to it. The binding is via the terminal nitrogen atom. At the same time, there is no appropriate UBI–QEP formula for calculating such binding of linear (or almost linear) triatomic molecules like $N_2O$ or $CO_2$.

**Table 6.** Binding energies of $N_2O$ (kcal/mol) calculated using different formulas

| Formula | Pt | Pd | Re | Rh | Ir | Ni | Au | Ag | Cu |
|---|---|---|---|---|---|---|---|---|---|
| (8), $n = 1$ | 14.4 | 17.7 | 20.7 | 14.4 | 17.0 | 18.9 | 10.4 | 11.0 | 14.2 |
| (9)–(10) | 12.2 | 17.1 | 13.3 | 9.2 | 14.0 | 12.4 | 8.3 | 8.2 | 9.0 |
| (9), (11), (12) | 9.8 | 13.1 | 12.4 | 8.6 | 11.3 | 11.3 | 6.8 | 6.9 | 8.4 |

The formula

$$Q_{N_2O,\perp} = \frac{Q_{0N}^2}{Q_{0N}/n + D_{N_2O}} \quad (8)$$

somewhat overestimates the binding energy. An alternative method is the use of the formula for binding via two nitrogen atoms or via the central nitrogen atom and oxygen. In this case, the binding energies are even higher, and the contributions of bond energies to $D_{N_2O}$ in the adsorbed nitrous oxide molecule have to be postulated. The best variant is the quasi-diatomic approximation, in which the $N_t$–$N_c$–O molecule is considered as diatomic N··O with the bond energy $D_{N_2O}$ = 266 kcal/mol, equal to the sum of N–O and N–N bond energies (subscripts t and c refer to the terminal and central nitrogen atoms). Then, the binding energy can be calculated by the formula

$$Q_{N\cdots O} = \frac{ab(a+b) + D_{N_2O}(a-b)^2}{ab + D_{N_2O}(a+b)}, \quad (9)$$

where

$$a = Q_{0N}^2(Q_{0N} + 2Q_{0O})/(Q_{0N} + Q_{0O})^2 \quad (10)$$

and

$$b = Q_{0O}^2(Q_{0O} + 2Q_{0N})/(Q_{0N} + Q_{0O})^2. \quad (11)$$

The use of this formula was recommended in [58], but it can be further improved [61]. The physical meaning of parameters $a$ and $b$ is as follows [62]: They take into account a decrease in $Q_{0N}$ and $Q_{0O}$ due to the repulsion between metal atom $M_N$ bound to N and atom O and the repulsion between metal atom $M_O$ bound to O and atom N ($M_N$–$N_t$··O–$M_O$). Formula (9) neglects the existence of the central nitrogen atom $N_c$ between $N_t$ and O ($M_N$–$N_t$–$N_c$–O–$M_O$). Because it is this atom that is the main source of repulsion from metal atoms, formula (9) overestimates the binding energy of $N_2O$. This limitation of formula (9) can be removed if $a$ is calculated for the $M_N$–$N_t$–$N_c$ fragment and $b$ is calculated for the $N_c$–O–$M_O$ fragment. Then, $a$ is determined by formula (12), which is obtained by replacing $Q_{0O}$ by $Q_{0N}$ in formula (11):

$$a = Q_{0N}^2(Q_{0N} + 2Q_{0N})/(Q_{0N} + Q_{0N})^2 = 0.75Q_{0N}. \quad (12)$$

The results of calculations of the binding energy using different formulas in the zero-coverage limit is shown in Table 6. Calculation using formula (9) assumes that the on-top position of $N_2O$ and, therefore, the results are applicable to all crystalline planes. Analysis of formula (9) shows that, with an increase in $n$, the binding energy increases and, therefore, the positions with a greater number of metal–nitrogen bonds should be preferable. However, as follows from the $N_2O$ desorption temperatures, lower values of binding energies are more realistic. In further calculations we used data obtained using formulas (9), (11), and (12).

### *Activation Energies of Reactions and Diffusion*

The UBI–QEP method makes it possible to calculate the activation energy of surface reactions [57]. To calculate the activation energy of a reaction of the type

$$AB_{ads} \longrightarrow A_{ads} + B_{ads},$$

the following formula is used:

$$E = \frac{1}{2}\left(\Delta H + \frac{Q_A Q_B}{Q_A + Q_B}\right), \quad (13)$$

where $\Delta H$ is the enthalpy of the surface reaction calculated from the thermodynamic cycle desorption–gas-phase reaction–adsorption:

$$\Delta H = Q_{AB} + D - Q_A - Q_B. \quad (14)$$

In this equation, $D$ is the enthalpy of an analogous gas-phase reaction estimated from the bond strengths:

$$D = D_{AB} - D_A - D_B. \quad (15)$$

The activation energy of the reverse reaction is calculated using the condition

$$E_f = E_r - \Delta H. \quad (16)$$

In the case of dissociation of linear triatomic molecules like $CO_2$ and $N_2O$, the following formula is used instead of formula (14) [56]:

$$E = \Delta H + \frac{Q_A Q_B}{Q_A + Q_B}, \quad (17)$$

in which there is no multiplier 1/2. The value of $E$ obtained in this way corresponds to the activation energy in the Lennard-Jones approximation.

If the activation energy is lower than zero, then a thermodynamic correction is introduced: this energy is

**Table 7.** Activation energies and enthalpies of reactions for three platinum surfaces (in kcal/mol)

| Reaction* | $D$** | Pt(111) | | | Pt(100) | | | Pt(110) | | |
|---|---|---|---|---|---|---|---|---|---|---|
| | | $E_{a,f}$ | $E_{a,r}$ | $\Delta H$ | $E_{a,f}$ | $E_{a,r}$ | $\Delta H$ | $E_{a,f}$ | $E_{a,r}$ | $\Delta H$ |
| $O + N_2 = NO + N$ | 75.0 | 27.0 | 0.0 | 27.0 | 24.5 | 0.0 | 24.5 | 23.4 | 0.4 | 23.0 |
| $NO + N_2 = N_2O + N$ | 111.0 | 23.9 | 0.0 | 23.9 | 19.0 | 0.0 | 19.0 | 16.1 | 0.0 | 16.1 |
| $2NO = N_2O + O$ | 36.0 | 2.8 | 5.9 | –3.1 | 1.7 | 7.1 | –5.5 | 1.0 | 7.8 | –6.8 |
| $O + NO = O_2 + N$ | 32.0 | 18.2 | 0.0 | 18.2 | 17.6 | 0.0 | 17.6 | 17.3 | 0.0 | 17.3 |
| $O_2 + N_2 = N_2O + O$ | 79.0 | 7.2 | 1.6 | 5.6 | 5.1 | 3.7 | 1.7 | 3.8 | 5.0 | –1.2 |
| $N_2 = 2N$ | 226.0 | 31.4 | 26.6 | 4.8 | 27.1 | 33.8 | –6.8 | 24.4 | 38.2 | –13.8 |
| $NO = O + N$ | 151.0 | 13.4 | 35.6 | –22.2 | 10.1 | 41.4 | –31.3 | 8.1 | 44.8 | –36.7 |
| $N_2O = NO + N$ | 115.0 | 3.4 | 22.4 | –19.1 | 0.0 | 25.8 | –25.8 | 0.0 | 29.9 | –29.9 |
| $N_2O = O + N_2$ | 40.0 | 0.0 | 46.1 | –46.1 | 0.0 | 50.3 | –50.3 | 0.0 | 52.9 | –52.9 |
| $O_2 = 2O$ | 119.0 | 1.0 | 41.5 | –40.4 | 0.0 | 48.9 | –48.9 | 0.0 | 54.0 | –54.0 |
| $(NO)_2 = 2NO$ | 3.0 | 5.2 | 13.9 | –8.7 | 3.8 | 14.4 | –10.6 | 2.9 | 14.7 | –11.8 |
| $(NO)_2 = N_2O + O$ | 39.0 | 0.0 | 11.8 | –11.8 | 0.0 | 16.1 | –16.1 | 0.0 | 18.6 | –18.6 |

* All molecules and atoms are surface species.
** $D$ is the enthalpy of the analogous gas-phase reaction.

**Table 8.** Activation energies and enthalpies of reactions for the (111) surfaces of nickel, palladium, and platinum (in kcal/mol)

| Reaction* | $D$** | Ni(111) | | | Pd(111) | | | Pt(111) | | |
|---|---|---|---|---|---|---|---|---|---|---|
| | | $E_{a,f}$ | $E_{a,r}$ | $\Delta H$ | $E_{a,f}$ | $E_{a,r}$ | $\Delta H$ | $E_{a,f}$ | $E_{a,r}$ | $\Delta H$ |
| $O + N_2 = NO + N$ | 75.0 | 32.5 | 0.0 | 32.5 | 19.2 | 8.0 | 11.2 | 27.0 | 0.0 | 27.0 |
| $NO + N_2 = N_2O + N$ | 111.0 | 16.0 | 0.0 | 16.0 | 15.7 | 0.0 | 15.7 | 23.9 | 0.0 | 23.9 |
| $2NO = N_2O + O$ | 36.0 | 0.0 | 16.6 | –16.6 | 7.9 | 3.4 | 4.5 | 2.8 | 5.9 | –3.1 |
| $O + NO = O_2 + N$ | 32.0 | 30.4 | 0.0 | 30.4 | 12.4 | 0.0 | 12.4 | 18.2 | 0.0 | 18.2 |
| $O_2 + N_2 = N_2O + O$ | 79.0 | 0.0 | 14.4 | –14.4 | 7.3 | 4.1 | 3.3 | 7.2 | 1.6 | 5.6 |
| $N_2 = 2N$ | 226.0 | 18.9 | 48.6 | –29.6 | 22.2 | 42.8 | –20.6 | 31.4 | 26.6 | 4.8 |
| $NO = O + N$ | 151.0 | 0.0 | 62.1 | –62.1 | 10.2 | 42.0 | –31.8 | 13.4 | 35.6 | –22.2 |
| $N_2O = NO + N$ | 115.0 | 0.0 | 45.6 | –45.6 | 0.0 | 36.3 | –36.3 | 3.4 | 22.4 | –19.1 |
| $N_2O = O + N_2$ | 40.0 | 0.0 | 78.1 | –78.1 | 0.0 | 47.5 | –47.5 | 0.0 | 46.1 | –46.1 |
| $O_2 = 2O$ | 119.0 | 0.0 | 92.5 | –92.5 | 0.0 | 44.2 | –44.2 | 1.0 | 41.5 | –40.4 |
| $(NO)_2 = 2NO$ | 3.0 | 2.1 | 16.3 | –14.2 | 4.6 | 17.2 | –12.6 | 5.2 | 13.9 | –8.7 |
| $(NO)_2 = N_2O + O$ | 39.0 | 0.0 | 30.7 | –30.7 | 3.3 | 11.4 | –8.1 | 0.0 | 11.8 | –11.8 |

* All molecules and atoms are surface species.
** $D$ is the enthalpy of the analogous gas-phase reaction.

set equal to zero, and the energy of the reverse reaction is set equal to the enthalpy.

The activation energy of the reaction

$$A_{ads} + BC_{ads} \longrightarrow AB_{ads} + C_{ads}$$

is calculated using the formulas

$$E = \frac{1}{2}\left(\Delta H + \frac{Q_{AB}Q_C}{Q_{AB} + Q_C}\right), \quad (18)$$

$$\Delta H = Q_A + Q_{BC} + D_{BC} - D_{AB} - Q_{AB} - Q_C. \quad (19)$$

The direction of the reaction is chosen from the condition for the corresponding bond energies $D_{BC} > D_{AB}$. Using these formulas, we calculated the activation energies of reactions on single-crystalline surfaces.

The results of calculations of the activation energies of forward ($E_{a,f}$) and reverse ($E_{a,r}$) reactions, as well as the enthalpies of reactions in the forward direction ($\Delta H$) for three platinum surfaces in the zero-coverage

**Table 9.** Activation energies and enthalpies of reactions for the surfaces of rhenium(0001), rhodium(111), and iridium(111) (kcal/mol)

| Reaction* | $D$** | Re(0001) | | | Rh(111) | | | Ir(111) | | |
|---|---|---|---|---|---|---|---|---|---|---|
| | | $E_{a,f}$ | $E_{a,r}$ | $\Delta H$ | $E_{a,f}$ | $E_{a,r}$ | $\Delta H$ | $E_{a,f}$ | $E_{a,r}$ | $\Delta H$ |
| $O + N_2 = NO + N$ | 75.0 | 33.4 | 0.0 | 33.4 | 44.0 | 0.0 | 44.0 | 23.5 | 2.6 | 20.9 |
| $NO + N_2 = N_2O + N$ | 111.0 | 12.9 | 0.0 | 12.9 | 25.1 | 0.0 | 25.1 | 18.5 | 0.0 | 18.5 |
| $2NO = N_2O + O$ | 36.0 | 0.0 | 20.5 | –20.5 | 0.0 | 18.9 | –18.9 | 3.8 | 6.2 | –2.4 |
| $O + NO = O_2 + N$ | 32.0 | 34.0 | 0.0 | 34.0 | 31.0 | 0.0 | 31.0 | 18.4 | 0.0 | 18.4 |
| $O_2 + N_2 = N_2O + O$ | 79.0 | 0.0 | 21.1 | –21.1 | 1.0 | 6.9 | –5.9 | 5.1 | 5.0 | 0.1 |
| $N_2 = 2N$ | 226.0 | 14.4 | 56.6 | –42.2 | 31.4 | 26.6 | 4.8 | 24.2 | 39.3 | –15.2 |
| $NO = O + N$ | 151.0 | 0.0 | 75.5 | –75.5 | 7.5 | 46.7 | –39.2 | 8.8 | 44.9 | –36.1 |
| $N_2O = NO + N$ | 115.0 | 0.0 | 55.0 | –55.0 | 2.2 | 22.4 | –20.2 | 0.0 | 33.7 | –33.7 |
| $N_2O = O + N_2$ | 40.0 | 0.0 | 88.4 | –88.4 | 0.0 | 64.2 | –64.2 | 0.0 | 54.6 | –54.6 |
| $O_2 = 2O$ | 119.0 | 0.0 | 109.5 | –109.5 | 0.0 | 70.2 | –70.2 | 0.0 | 54.5 | –54.5 |
| $(NO)_2 = 2NO$ | 3.0 | 1.9 | 18.3 | –16.5 | 2.6 | 11.3 | –8.7 | 2.4 | 14.1 | –11.7 |
| $(NO)_2 = N_2O + O$ | 39.0 | 0.0 | 37.0 | –37.0 | 0.0 | 27.6 | –27.6 | 0.0 | 14.1 | –14.1 |

* All molecules and atoms are surface species.
** $D$ is the enthalpy of the analogous gas-phase reaction.

**Table 10.** Activation energies and enthalpies of reactions for the (111) surfaces of copper, silver, and gold (kcal/mol)

| Reaction* | $D$** | Cu(111) | | | Ag(111) | | | Au(111) | | |
|---|---|---|---|---|---|---|---|---|---|---|
| | | $E_{a,f}$ | $E_{a,r}$ | $\Delta H$ | $E_{a,f}$ | $E_{a,r}$ | $\Delta H$ | $E_{a,f}$ | $E_{a,r}$ | $\Delta H$ |
| $O + N_2 = NO + N$ | 75.0 | 46.3 | 0.0 | 46.3 | 42.1 | 0.0 | 42.1 | 40.8 | 0.0 | 40.8 |
| $NO + N_2 = N_2O + N$ | 111.0 | 25.5 | 0.0 | 25.5 | 33.3 | 0.0 | 33.3 | 34.7 | 0.0 | 34.7 |
| $2NO = N_2O + O$ | 36.0 | 0.0 | 20.7 | –20.7 | 0.0 | 8.8 | –8.8 | 0.1 | 6.2 | –6.1 |
| $O + NO = O_2 + N$ | 32.0 | 32.3 | 0.0 | 32.3 | 23.6 | 0.0 | 23.6 | 21.5 | 0.0 | 21.5 |
| $O_2 + N_2 = N_2O + O$ | 79.0 | 0.6 | 7.3 | –6.7 | 9.7 | 0.0 | 9.7 | 13.2 | 0.0 | 13.2 |
| $N_2 = 2N$ | 226.0 | 32.1 | 25.4 | 6.6 | 42.1 | 7.9 | 34.1 | 44.1 | 4.4 | 39.7 |
| $NO = O + N$ | 151.0 | 7.3 | 47.0 | –39.6 | 18.2 | 26.2 | –7.9 | 20.6 | 21.7 | –1.1 |
| $N_2O = NO + N$ | 115.0 | 3.2 | 22.1 | –18.9 | 18.2 | 17.4 | 0.9 | 21.5 | 16.5 | 5.0 |
| $N_2O = O + N_2$ | 40.0 | 0.0 | 65.2 | –65.2 | 0.0 | 41.2 | –41.2 | 0.0 | 35.9 | –35.9 |
| $O_2 = 2O$ | 119.0 | 0.0 | 71.9 | –71.9 | 4.2 | 35.8 | –31.5 | 7.4 | 30.1 | –22.6 |
| $(NO)_2 = 2NO$ | 3.0 | 2.6 | 11.1 | –8.4 | 2.8 | 7.8 | –5.0 | 2.8 | 7.2 | –4.4 |
| $(NO)_2 = N_2O + O$ | 39.0 | 0.0 | 29.2 | –29.2 | 0.0 | 13.8 | –13.8 | 0.0 | 10.5 | –10.5 |

* All molecules and atoms are surface species.
** $D$ is the enthalpy of the analogous gas-phase reaction.

limit, are summarized in Table 7. As can be seen from these data, there is no qualitative difference between various surfaces of the same metal at low coverages. The reaction of $N_2O$ decomposition occurs equally readily on all surfaces. The energetics of elementary reactions at zero coverages cannot explain the structural sensitivity. The results for Pd(111), Ni(111), Re(0001), Rh(111), Ir(111), Cu(111), Ag(111), and Au(111) are shown in Tables 8–10.

These theoretical data shed some light on the possible pathways of $N_2O$ formation from NO (the activation energies in kcal/mol are shown under the arrows):

$$NO_{ads} + NO_{ads} \xrightarrow{18.2} NO_{ads} + N_{ads}$$

$$+ O_{ads} \xrightarrow{9.4} N_2O_{ads} + O_{ads},$$

$$NO_{ads} + NO_{ads} \xrightarrow{7.8} (NO)_{2,ads} \xrightarrow{5.0} N_2O_{ads} + O_{ads},$$

**Table 11.** Comparison of calculated and experimental values of the adsorption heats of $N_2O$ at low coverages

| Surface | Parameter | Ref. | Experimental value, kcal/mol | UBI–QEP value, kcal/mol |
|---|---|---|---|---|
| Pt(111) | $Q_{N_2O}$ | [9] | 6 | 9.8 |
| Pd(110) | $Q_{N_2O}$ | [63] | 8.3 | 13.1 |
| Pd(110) | $E_d$–$E_{diss}$ | [14] | 3.3 | 13.1 |
| Ni(110) | $E_d$–$E_{diss}$ | [19] | 3.7 | 11.3 |
| Ni(100) | $Q_{N_2O}$ | [28] | 6.2 | 11.3 |
| Ni(100) | $E_{diss}$ | [28] | 2.5 | 0 |
| Cu(111) | $E_d$–$E_{diss}$ | [12] | 10.4 | 8.4 |
| Cu(100) | $Q_{N_2O}$ | [43] | <6 | 8.4 |
| Cu(110) | $E_d$–$E_{diss}$ | [39] | 2 | 8.4 |

$$NO_{ads} + NO_{ads} \xrightarrow{0.0} N_2O_{ads} + O_{ads}.$$

Of the three possible pathways of this reactions on the Ag(111) surface at low surface coverages, the direct formation of $N_2O$ from two NO molecules is the most probable. In the case of $N_2O_{ads}$ formation via the dimer $(NO)_{2,\,ads}$, the activation energies of both steps are rather low. In the case of $N_2O$ formation from $NO_{ads}$ and $N_{ads}$, the dissociation of $NO_{ads}$ requires overcoming a rather high barrier (18.2 kcal/mol). It should be taken into account that the direct formation of nitrous oxide is limited by the surface diffusion of NO, and the activation energy can be estimated by the following formula in this case [57]:

$$E_{diff,\,NO} = Q_{NO}\frac{n-2}{4n-2} = Q_{NO}/10 \quad (\text{at } n = 3).$$

For NO adsorbed on Ag(111), this value is 2.1 kcal/mol. However, the channel of the reaction via dimer formation may start to play a more important role at higher surface coverages. On other metals, the situation is qualitatively the same.

Table 11 compares the results of calculations and experimental data obtained for the low surface coverages. The experimental values of $Q_{N_2O}$ and the values of the difference of the activation energy of $N_2O$ desorption and its dissociation on the surface ($E_d$–$E_{diss}$) should coincide, taking into account that the activation energy of dissociation is equal to zero at zero coverages. As can be seen, the agreement between the various experimental data is not good. Therefore, it is difficult to judge the correctness of the theoretical estimates.

## CONCLUSIONS

Although substantial experimental information on the interaction of nitrous oxide with transition metal surfaces has been accumulated, several questions remain open. Specifically, the structural sensitivity of nitrous oxide decomposition cannot be explained by the difference in the energetics of adsorption. Mechanisms proposed for this process do not describe well the experimental data for single-crystal surfaces. The nature of two precursors in nitrous oxide dissociation remains unclear. It is also unclear why rather favorable dissociation reaction of $N_2O$ into $NO_{ads}$ and $O_{ads}$ does not occur competitively with the main reaction of dissociation into molecular nitrogen and $O_{ads}$. Data on the geometry of nitrous oxide adsorption are rather contradictory, and we do not know how this molecule coordinates to the surface. More detailed studies of energetics of this reaction for various surface coverages and microkinetic modeling of $N_2O$ dissociation would possibly shed light on these issues.

## ACKNOWLEDGMENTS

I am grateful to Professor E. Shustorovich for fruitful discussions and useful remarks.

## REFERENCES

1. Leont'ev, A.V., Fomicheva, O.A., Proskurina, M.V., and Zefirov, N.S., *Usp. Khim.*, 2001, vol. 70, p. 107.
2. Kapteijn, F., Rodriguez-Mirasol, J., and Moulijn, J.A., *Appl. Catal., B*, 1997, vol. 9, p. 25.
3. Kharitonov, A.S., Sobolev, V.I., and Panov, G.I., *Usp. Khim.*, 1992, vol. 61, p. 2062.
4. Brown, W.A. and King, D.A., *J. Phys. Chem. B*, 2000, vol. 104, p. 2578.
5. Cornish, J.C.L. and Avery, N.R., *Surf. Sci.*, 1990, vol. 235, p. 209.
6. Schwaner, A.L., Mahmood, W., and White, J.M., *Surf. Sci.*, 1996, vol. 351, p. 228.
7. Ceballos, C., Wende, H., Baberschke, K., and Arvanitis, D., *Surf. Sci.*, 2001, vols. 482–485, p. 15.
8. Väterlein, P., Krause, T., Bäßler, M., Fink, R., Umbach, E., Taborski, J., Wüstenhagen, V., and Wurth, W., *Phys. Rev. Lett.*, 1996, vol. 76, p. 4749.
9. Avery, N.R., *Surf. Sci.*, 1983, vol. 131, p. 501.
10. Kiss, J., Lennon, D., Jo, S.K., and White, J.M., *J. Chem. Phys.*, 1991, vol. 95, p. 8054.

11. Beck, D.E., Hetzinger, J.M., Avoyan, A., and Koel, B.E., *Surf. Sci.*, 2001, vol. 491, p. 48.
12. Habraken, F.H.P.M., Kieffer, E.Ph., and Bootsma, G.A., *Surf. Sci.*, 1979, vol. 83, p. 45.
13. Spitzer, A. and Luth, H., *Phys. Rev. B: Condens. Matter*, 1984, vol. 30, p. 3098.
14. Haq, S. and Hodgson, A., *Surf. Sci.*, 2000, vol. 463, p. 1.
15. Horino, H., Liu, S., Hiratsuka, A., Ohno, Y., and Matsushima, T., *Chem. Phys. Lett.*, 2001, vol. 341, p. 419.
16. Ohno, Y., Kobal, I., Horino, H., Rzeznicka, I., and Matsushima, T., *Appl. Surf. Sci.*, 2001, vols. 169–170, p. 273.
17. Carabineiro, S.A. and Nieuwenhuys, B.E., *Surf. Sci.*, 2001, vol. 495, p. 1.
18. Li, Y. and Bowker, M., *Surf. Sci.*, 1996, vol. 348, p. 67.
19. Sau, R. and Hudson, J.B., *J. Vac. Sci. Technol.*, 1981, vol. 18, p. 607.
20. Arlow, J.S. and Woodruff, D.P., *Surf. Sci.*, 1985, vol. 162, p. 310.
21. Arlow, J.S. and Woodruff, D.P., *Surf. Sci.*, 1985, vol. 162, p. 327.
22. Kim, Y., Schreifels, J.A., and White, J.M., *Surf. Sci.*, 1982, vol. 114, p. 349.
23. Madey, T.E., Avery, N.R., Anton, A.B., Toby, B.H., and Weinberg, W.H., *J. Vac. Sci. Technol., A*, 1983, vol. 1, p. 1220.
24. Umbach, E. and Menzel, D., *Chem. Phys. Lett.*, 1981, vol. 84, p. 491.
25. Huang, H.H., Seet, C.S., Zou, Z., and Xu, G.Q., *Surf. Sci.*, 1996, vol. 356, p. 181.
26. Daniel, W.M., Kim, Y., Peebles, H.C., and White, J.M., *Surf. Sci.*, 1981, vol. 111, p. 189.
27. Onchu, M. and Farnsworth, H.E., *Surf. Sci.*, 1969, vol. 13, p. 424.
28. Hoffman, D.A. and Hudson, J.B., *Surf. Sci.*, 1987, vol. 180, p. 77.
29. Kodama, C., Orita, H., and Hozoye, H., *Appl. Surf. Sci.*, 1997, vols. 121/122, p. 579.
30. Redmond, J.P., *J. Catal.*, 1967, vol. 7, p. 297.
31. Redmond, J.P., *J. Phys. Chem.*, 1963, vol. 67, p. 788.
32. Riekert, L. and Staib, M., *Ber. Bunsen-Ges. Phys. Chem.*, 1963, vol. 67, p. 976.
33. Barker, F.G. and Gasser, R.P.H., *Surf. Sci.*, 1973, vol. 39, p. 136.
34. Gasser, R.H.H. and Marsey, C.J., *Surf. Sci.*, 1970, vol. 20, p. 116.
35. Uetsuka, H., Aoyagi, K., Tanaka, S., Yuzaki, K., Ito, S., Kameoka, S., and Kunimori, K., *Catal. Lett.*, 2000, vol. 66, p. 87.
36. Fuggle, J.C. and Menzel, D., *Surf. Sci.*, 1979, vol. 79, p. 1.
37. Weinberg, W.H. and Merrill, R.P., *Surf. Sci.*, 1972, vol. 32, p. 317.
38. Klein, R. and Siegel, R., *Surf. Sci.*, 1980, vol. 92, p. 337.
39. Habraken, F.H.P.M. and Bootsma, G.A., *Surf. Sci.*, 1979, vol. 87, no. 2, p. 333.
40. Onchi, M. and Farnsworth, H.E., *Surf. Sci.*, 1969, vol. 13, p. 424.
41. Klein, R. and Siegel, R., *Surf. Sci.*, 1980, vol. 92, p. 337.
42. Masel, R.I., Umbach, E., Fuggle, J.C., and Menzel, D., *Surf. Sci.*, 1979, vol. 79, p. 26.
43. Johnson, D.W., Watloob, M.H., and Roberts, M.W., *J. Chem. Soc., Chem. Commun.*, 1978, no. 2, p. 40.
44. Dumas, P., Suren, M., Chabal, Y.J., Hirschmugl, C.J., and Williams, G.P., *Surf. Sci.*, 1997, vol. 371, p. 200.
45. So, S.K., Franchy, R., and Ho, W., *J. Chem. Phys.*, 1989, vol. 91, p. 5701.
46. So, S.K., Franchy, R., and Ho, W., *J. Chem. Phys.*, 1991, vol. 95, p. 1385.
47. Nelin, C.J., Bagus, P.S., Behm, R.J., and Brundle, C.R., *Chem. Phys. Lett.*, 1984, vol. 105, p. 58.
48. Behm, R.J. and Brundle, C.R., *J. Vac. Sci. Tech. A*, 1984, vol. 2, p. 1040.
49. Brown, W.A., Gardner, P., and King, D.A., *J. Phys. Chem.*, 1995, vol. 99, p. 7065.
50. Brown, W.A., Gardner, P., Perez Jigato, M., and King, D.A., *J. Chem. Phys.*, 1995, vol. 102, p. 7277.
51. Ohno, Y., Kimura, K., Bi, M., and Matsushima, T., *J. Chem. Phys.*, 1999, vol. 110, p. 8221.
52. Sharpe, R.G. and Bowker, M., *Surf. Sci.*, 1996, vol. 360, p. 21.
53. Jansch, H.J., Huang, C., Ludviksson, A., Rocker, G., Redding, J.D., Metiu, H., and Martin, R.M., *Surf. Sci.*, 1989, vol. 214, p. 377.
54. Scholten, J.J.F., Konvalinka, J.A., and Beekman, F.W., *J. Catal.*, 1973, vol. 28, p. 209.
55. Shi, S.-K. and White, J.M., *J. Chem. Phys.*, 1980, vol. 73, p. 5889.
56. Shustorovich, E., *Adv. Catal.*, 1990, vol. 37, p. 101.
57. Shustorovich, E. and Sellers, H., *Surf. Sci. Rep.*, 1998, vol. 31, p. 1.
58. Sellers, H. and Shustorovich, E., *Surf. Sci.*, 2002, vol. 504, p. 167.
59. Irokawa, K., Arai, H., Kobayashi, J., Kioka, T., Sugai, S., Miki, H., and Kato, H., *Surf. Sci.*, 1996, vols. 357/358, p. 274.
60. Rice, O.K., *J. Chem. Phys.*, 1936, vol. 4, p. 367.
61. Shustorovich, E., private communication.
62. Shustorovich, E., *Surf. Sci.*, 1987, vol. 181, p. 205.
63. Kokalj, A., Kobal, I., Horino, H., Ohno, Y., and Matsushima, T., *Surf. Sci.*, 2002, vol. 506, p. 196.